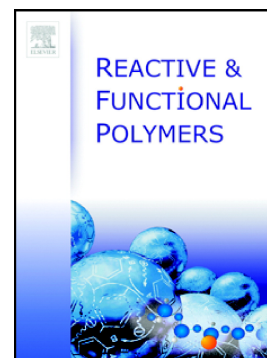


Accepted Manuscript

Microporous frameworks based on adamantane building blocks: Synthesis, porosity, selective adsorption and functional application

Xiong Li, Jianwei Guo, Rui Tong, Paul D. Topham, Jiawei Wang



PII: S1381-5148(18)30383-3
DOI: [doi:10.1016/j.reactfunctpolym.2018.06.008](https://doi.org/10.1016/j.reactfunctpolym.2018.06.008)
Reference: REACT 4064
To appear in: *Reactive and Functional Polymers*
Received date: 23 April 2018
Revised date: 15 June 2018
Accepted date: 17 June 2018

Please cite this article as: Xiong Li, Jianwei Guo, Rui Tong, Paul D. Topham, Jiawei Wang , Microporous frameworks based on adamantane building blocks: Synthesis, porosity, selective adsorption and functional application. *React* (2018), doi:[10.1016/j.reactfunctpolym.2018.06.008](https://doi.org/10.1016/j.reactfunctpolym.2018.06.008)

This is a PDF file of an unedited manuscript that has been accepted for publication. As a service to our customers we are providing this early version of the manuscript. The manuscript will undergo copyediting, typesetting, and review of the resulting proof before it is published in its final form. Please note that during the production process errors may be discovered which could affect the content, and all legal disclaimers that apply to the journal pertain.

Microporous frameworks based on adamantane building blocks: synthesis, porosity, selective adsorption and functional application

Xiong Li^a, Jianwei Guo^{a*}, Rui Tong^b, Paul D Topham^{c*}, Jiawei Wang^c

^aSchool of Chemical Engineering and Light Industry, Guangdong University of Technology, Guangzhou, 510006, China.

^bGuangzhou Tinci Materials Technology Co., Ltd., Guangzhou, 510760, China.

^cAston Institute of Materials Research, Aston University, Birmingham, B4 7ET, UK.

*Corresponding Authors

E-mail: guojw@gdut.edu.cn.

E-mail: p.d.topham@aston.ac.uk.

ACCEPTED MANUSCRIPT

Abstract: Two microporous organic frameworks based on adamantane (hereafter denoted as **MF-Ads**) were fabricated through Sonogashira-Hagihara coupling polycondensation of aryl halides and alkynes. Results show that both types of **MF-Ad** networks had similar porous properties and exhibited excellent CO₂ uptake capacity (72.5 cm³ g⁻¹) and CO₂/N₂ selectivity (59.1) at 273 K and 1.0 bar. Taking advantage of the superhydrophobic wettability of the resulting **MF-Ad** networks, wire mesh scaffolds were used to fabricate superhydrophobic films with polydimethylsiloxane (PDMS) acting as a binder. These films displayed excellent instant hydrocarbon/water separation efficiency (up to 99.6 %), which was maintained at a constant level after five repeated cycles. This work provides a novel insight into the fabrication of microporous organic frameworks and extends their applicability to carbon capture and absorption of hazardous organic pollutants.

Keywords: microporous frameworks, selectivity, superhydrophobic, wettability, separation efficiency

ACCEPTED MANUSCRIPT

1. Introduction

During the past decade, considerable research effort has been devoted to the development of advanced materials for capturing CO₂ efficiently, adsorbing hazardous organic pollutants and preventing further decline of our environment[1-3]. Work has recently revealed that most frameworks with abundant porous structure, such as metal organic frameworks (MOFs)[4], covalent organic frameworks (COFs)[5] and microporous organic polymers (MOPs)[6], to name a few, are promising adsorbents for capturing CO₂ due to their remarkably high surface area, large adsorption capacity and tunable chemical composition. Interestingly, in contrast to most reported MOFs and COFs which commonly suffer from poor chemical and thermal stabilities, MOPs are fabricated through C-C covalent bonds which provide better thermal and physicochemical stability. These improved properties make MOPs more suitable candidates than MOFs and COFs for carbon capture and storage (CCS) at high temperatures or in harsh environments[7, 8]. For example, Woo and Manoranjan synthesized a zo-linked polymers with ultrahigh CO₂ adsorption capacity (up to 195 mg g⁻¹) with a weight loss of 10 % up to between 280 and 305 °C, depended on the network[9]. Kundu and Bhaumik reported a nitrogen- and sulfur-rich hyper-cross-linked microporous poly(triazine-thiophene) copolymer (HMC-1), which exhibited a CO₂ uptake of 462 mg g⁻¹ at 273 K and 3.0 bar, but gave a weight loss of 10 % at 220 °C[1]. Conversely, for reported MOPs, Janiak *et al.* carried out a mixed-linker approach to obtain a triazine-based framework (Ad2L1), which had good CO₂ adsorption capacity (77.3 mg g⁻¹ at 273 K and 1.0 bar) and CO₂/N₂ selectivity (up to 13). Importantly, the Ad2L1 framework showed remarkable thermal stability (stable up to 400 °C)[10]. Chang *et al.* reported microporous hydrocarbon particles based on adamantane building blocks, which exhibited high BET surface area (up to 665 m² g⁻¹) and narrow pore size distribution (0.6 nm)[11]. Zulfiqar *et al.* synthesized a nanoporous amide network based on tetraphenyladamantane (NAN-1), which exhibited ultrahigh thermal stability (stable up to 500 °C) and good CO₂ adsorption capacity (55.7 mg g⁻¹ at 273 K and 1.0 bar)[12]. These excellent physicochemical and hydrothermal stabilities may be attributed to the exclusively aromatic structure and the sole presence of C-C covalent bonds within the framework of these MOP materials[13, 14]. However, compared with MOFs and COFs, most of reported MOPs typically exhibit higher thermal stability but with lower CO₂ adsorption capacity and selectivity over N₂. Furthermore, the large adsorption capacity of microporous frameworks is another significant parameter for their use in CCS. Therefore, there is a need, yet significant challenge, to develop new strategies to synthesize MOPs with higher CO₂ adsorption capacity and selectivity over N₂.

On the other hand, to date, all of the reported microporous organic polymers are found in powder form with poor processability, which has severely limited their application in gas storage/separation. The development of MOPs with better processability and chemical inertness is beneficial to expand the potential of these microporous frameworks. Recently a small number of novel strategies has received great attention to tackle these challenges [15-18]. However, it is still difficult to fully address these limitations for any industrial application due to the inefficiency of these strategies.

With these considerations in mind, herein, we report the synthesis of microporous frameworks based on adamantane (**MF-Ad-1** and **MF-Ad-2**) *via* Sonogashira-Hagihara coupling between 4,4'-diethynylbiphenyl and aryl halides. The gas-adsorption properties of these microporous frameworks have been evaluated and exhibit excellent selectivity for CO₂ over N₂. More interestingly, these microporous frameworks also showed superhydrophobicity when coated with polydimethylsiloxane (PDMS), which were particularly useful for the separation of hydrocarbons/water. These studies elegantly extend the applications of microporous organic frameworks, particularly in CCS and adsorbing hazardous organic pollutants.

2. Experimental

2.1 Materials

Unless otherwise stated, all starting materials were purchased from Guoyao Chemical Reagent Co., Ltd. (China). Tetrahydrofuran (THF, anhydrous, 99.5 %), triethylamine (TEA, anhydrous, 99.5 %), dimethyl formamide (DMF, anhydrous, 99 %), toluene (99 %) and rhodamine B (99 %) were purchased from Shanghai Macklin Biochemical Co., Ltd. (China). 1,3-Dibromobenzene (anhydrous, 99.5%), 2-methyl-3-butyn-2-ol, 4,4'-dibromobiphenyl, copper(I) iodide [CuI], tetrakis(triphenylphosphine)palladium(0) [Pd(PPh₃)₄] and dichlorobis(triphenylphosphine)palladium(II) [Pd(PPh₃)₂Cl₂] were all purchased from Sigma-Aldrich Co., Ltd. (UK). 4,4'-diethynylbiphenyl (**DPE**) was synthesized according to the published method except that 2-methyl-3-butyn-2-ol was used instead of trimethylsilylacetylene[6]. 3,3',5,5',7,7'-Hexakis(4-bromophenyl)-1,1'-biadamantane (**HBPBA**) was synthesized according to published methods[19]. The PDMS (Sylgard 184) was obtained from Dow Corning Co., Ltd. (China). The stainless-steel meshes (30 mm × 40 mm) with a mesh opening size of 0.55 mm were obtained from Anping Park Lin Metal Wire Mesh Co., Ltd. (China). The stainless-steel meshes were pretreated by washing with hydrochloric acid (2.0 M), water and acetone for three times and then dried at 80 °C.

2.2 Synthesis of 1,3,5,7-tetrakis(1,3-bromophenyl)adamantane (TBBPA).

1,3-dibromobenzene (70 ml) was added to a mixture of 1,3,5,7-tetrabromoadamantane (5.0 g, 11.1 mmol) and AlCl_3 powder (4.0 g, 30.0 mmol), at 0 °C. The mixture was then stirred at ambient temperature for 36 h. After quenching the reaction by adding ice water, the organic layer was diluted with chloroform and filtered. The filtrate was washed with deionised water and brine and then dried over magnesium sulfate. After evaporation to remove volatiles, 1,3,5,7-tetrakis(1,3-bromophenyl)adamantane was obtained as a white solid from the crystallization in chloroform (9.6 g, 81 % yield). ^1H NMR ($\text{DMSO}-d_6$, 400 MHz): δ (ppm) 7.80 (s, 8H), 7.69 (s, 4H), 2.05 (s, 12H); ^{13}C NMR (CDCl_3-d_3 , 400 MHz): δ (ppm) 150.7, 131.5, 126.2, 122.4, 45.3, 38.3. Anal. Calcd for $\text{C}_{34}\text{H}_{24}\text{Br}_8$: C, 38.10; H, 2.26; Found: C, 38.11; H, 2.21.

2.3 Synthesis of networks MF-Ad-1 and MF-Ad-2

For **MF-Ad-1**, a mixture of HBPBA (480.0 mg, 0.4 mmol), DPE (242.4 mg, 1.2 mmol), $\text{Pd}(\text{PPh}_3)_2\text{Cl}_2$ (28.1 mg, 0.04 mmol), CuI (152.4 mg, 0.08 mmol), dimethyl formamide (DMF) (60 ml) and triethylamine (TEA) (60 ml) were stirred in a 250 ml Schlenk flask and then heated to 90 °C for 48 h under argon atmosphere. After cooling to ambient temperature, the mixture was filtered, and the precipitate was washed with hot THF, DMF, 2.0 M hydrochloric acid, 2.0 M sodium hydroxide, water and methanol in succession. Importantly, the polymer was rigorously stirred at 2000 rpm during acid and base immersions for 30 min and the process was repeated 3 times. After filtration, the insoluble powder was dried under vacuum at 100 °C for at least 24 h to give **MF-Ad-1** (492 mg, 93 % yield) as a light yellow fluffy powder. Anal. Calcd for $\text{C}_{104}\text{H}_{72}$: C, 94.54; H, 5.46. Found: C, 92.12; H, 5.75.

The synthetic procedure of **MF-Ad-2** was similar to that of **MF-Ad-1**, except that the linker (knot) used was TBBPA (321.6 mg, 0.3 mmol), instead of HBPBA (480.0 mg, 0.4 mmol), which also afforded a light yellow fluffy powder (382 mg, 94 % yield). Anal. Calcd for $\text{C}_{80}\text{H}_{54}$: C, 94.67; H, 5.33. Found: C, 91.83; H, 5.57.

2.4 Preparation of superhydrophobic MF-Ad-based mesh films.

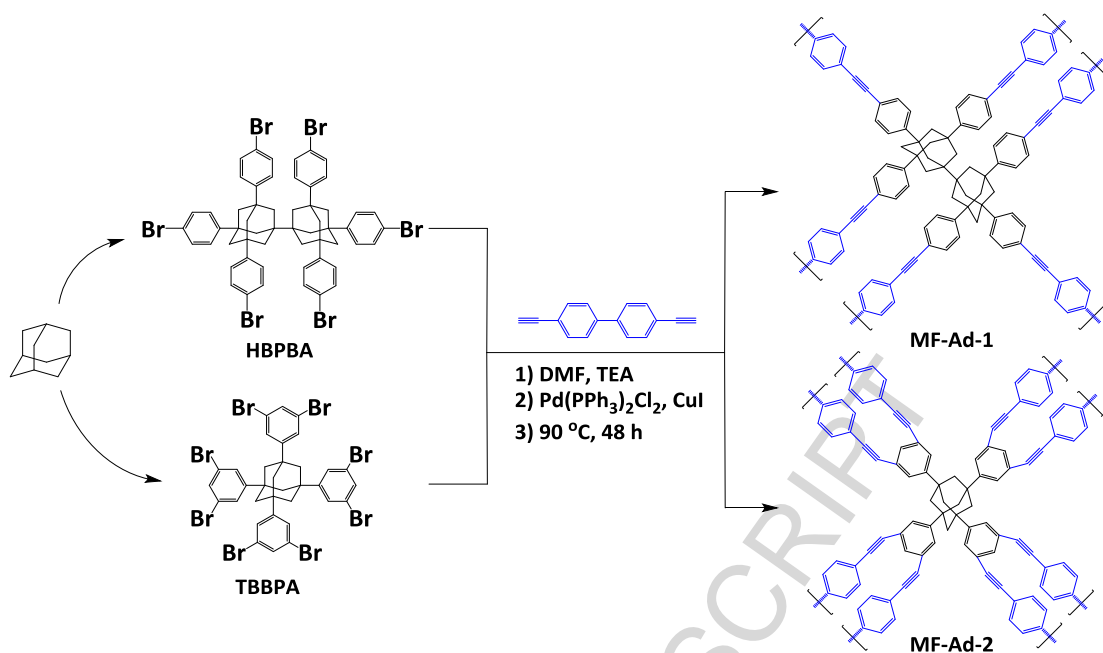
The following is an example for **MF-Ad-1**: **MF-Ad-1** (0.2 g) was added to a mixture of PDMS and toluene (at a total ratio of PDMS/toluene/**MF-Ad-1** of 1.1/10/0.2, w/w/w), at room temperature, and then the mixture was treated by ultrasonic tip-sonication for 30 min. A stainless-steel mesh was immersed into the mixture, dried at 85 °C, then repeated 20 times until the **MF-Ad**-based mesh films had successfully formed.

2.5 Characterization

Fourier transform infrared (FTIR) spectra were obtained using a Thermo Electron Nicolet-6700 spectrometer. ^1H NMR, ^{13}C NMR and solid-state cross polarization magic angle spinning (CP/MAS) NMR spectra were recorded on a Bruker AVANCE III 400 MHz Superconducting Fourier in deuterated chloroform (CDCl_3) or dimethyl sulfoxide- d_6 ($\text{DMSO}-d_6$). Powder X-ray diffraction (XRD) data were collected on a Bruker X'pertpro multipurpose diffractometer (MPD). Samples were mounted on a sample holder and measured using $\text{Cu K}\alpha$ radiation with 2θ range of 5° to 70°. Thermogravimetric analysis (TGA) was performed in a nitrogen atmosphere on a NETZSCH STA 409 PC thermal analyzer with a heating rate of 10 °C min^{-1} from ambient temperature to 800 °C. The nitrogen adsorption-desorption isotherms were measured on a 3H-2000PM2 analyzer and the adsorption of hydrogen, methane and carbon dioxide was measured on 3H-2000PS2 apparatus at 77 K/1.0 bar (H_2) and 273 K/1.0 bar (N_2 , CH_4 and CO_2). SEM analysis was performed on a Hitachi S-3400N scanning electron microscope to investigate the surface morphology of the polymers. Elemental analysis was performed with a Perkin Elmer Series II 2400 elemental analyzer. All samples were dried at 100 °C for 24 h under vacuum prior to measurement.

3. Results and discussion

The synthesis of two microporous organic frameworks, **MF-Ad-1** and **MF-Ad-2**, was accomplished via $\text{Pd}(0)/\text{CuI}$ -catalyzed Sonogashira-Hagihara cross coupling polymerization. These frameworks were constructed using two different 3D building links (or 'knots'), HBPBA and TBBPA, as illustrated in Scheme 1. All of the building units dissolved in the solvent, leading to good yields (93 % for **MF-Ad-1** and 94 % for **MF-Ad-2**) under mild reaction conditions. After the reaction, however, these frameworks were found to be insoluble in conventional organic solvents, such as methanol, chloroform and tetrahydrofuran, suggesting the formation of crosslinked structures.



Scheme 1 Synthetic routes to the **MF-Ad-1** and **MF-Ad-2** networks.

3.1 Structural characterization

¹H NMR and ¹³C NMR spectra (Figures S1 and S2, ESI) indicate the successful synthesis of the building knot (TBBPA). Additionally, the molecular structure of the **MF-Ad** networks was confirmed by FTIR and ¹³C CP/MAS solid-state NMR spectroscopies. As shown in Figure 1, the two **MF-Ad** networks showed bands at 3031 and 1599 cm⁻¹, arising from aromatic C=C stretching. The broad band at 3440 cm⁻¹ is attributed to the C-H groups from the C≡CH end-groups in the frameworks. The band at 2853 cm⁻¹ is characteristic of the C-H stretching vibrations of adamantane, whereas the bands occurring at 2203 cm⁻¹ for both **MF-Ad-1** and **MF-Ad-2** can be assigned to C≡C triple-bond stretching in the networks and those at 1908 cm⁻¹ are attributed to the C≡CH from the end-groups in the **MF-Ad** networks.

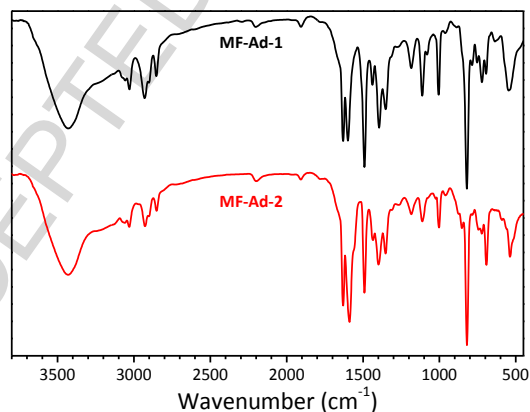


Figure 1. FTIR spectra of the **MF-Ad-1** and **MF-Ad-2** networks.

¹³C cross-polarization magic-angle spinning (CP/MAS) NMR spectroscopy was carried out to further confirm the structure of these **MF-Ad** networks (Figure S3, ESI). In the case of **MF-Ad-2**, the spectra showed peaks at 148.7, 138.8, 130.5, 125.8 and 123.2 ppm, assigned to the substituted phenyl carbons. The ethynylene units are observed at 90.6 ppm and the peaks at 47.3 and 38.5 ppm correspond to the adamantane carbons. All of the peaks in the **MF-Ad** networks are in good agreement with previous reports on similar networks, which were prepared from 1,3,5,7-tetrakis(4-iodophenyl)adamantane and 1,4-diethynylbenzene[11].

The broad feature in the XRD profiles (Figure S4, ESI) indicate that these two **MF-Ad** networks are amorphous in nature and therefore it is difficult to predict the actual framework of these **MF-Ad** networks, without diffraction peaks arising from a regular network with long range order. However, the sharper peak located at $2\theta \sim 43^\circ$ (d -spacing = 2.10 Å), which is assigned to disordered π - π stacking of the consecutive phenyl

rings[12], as well as the interlayer distance of the chiral helical frameworks in the ordered sections. Namely, these two **MF-Ad** frameworks have some degree of order through dispersed π - π stacking of the aromatic units (which is more prevalent in MF-Ad-2), but primarily comprise amorphous frameworks[20, 21]. SEM was used to examine the surface morphology of the two **MF-Ad** networks (Figure 2). **MF-Ad-1** consists of more discrete, agglomerated spherical entities while **MF-Ad-2** shows a more interconnected particulate framework.

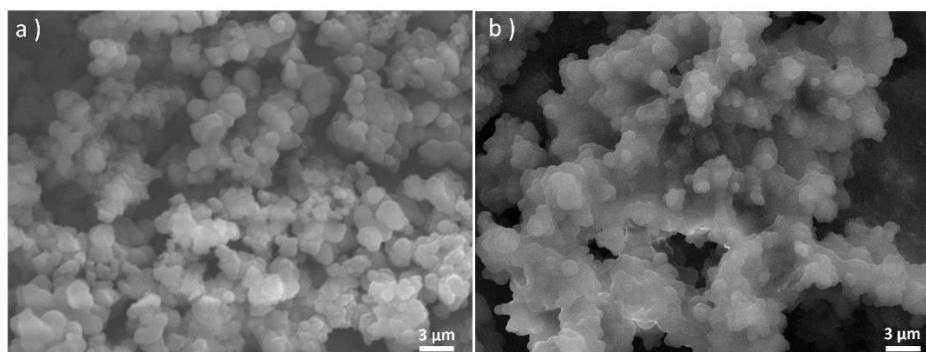


Figure 2. SEM images of **MF-Ad-1** (a) and **MF-Ad-2** (b).

3.2 Stability and porosity of MF-Ad networks

The thermogravimetric analysis (TGA) of as-prepared **MF-Ad** networks (Figure 3) showed a weight loss of 5% at 395 and 408 °C for **MF-Ad-1** and **MF-Ad-2**, respectively, under a nitrogen atmosphere [notably, the vast majority of the networks (80%) remained in place up to the end of the thermal analysis, *i.e.* 800 °C]. Additionally, the **MF-Ad** networks exhibited not only stability in common organic solvents but remained intact after immersion in both 2.0 M hydrochloric acid and sodium hydroxide (the FTIR spectra in Figure S5, ESI), demonstrating their excellent chemical stability. The ultra-high thermochemical stabilities of these frameworks are desired for applications in harsh conditions, such as the adsorption of acidic or alkaline waste gas streams.

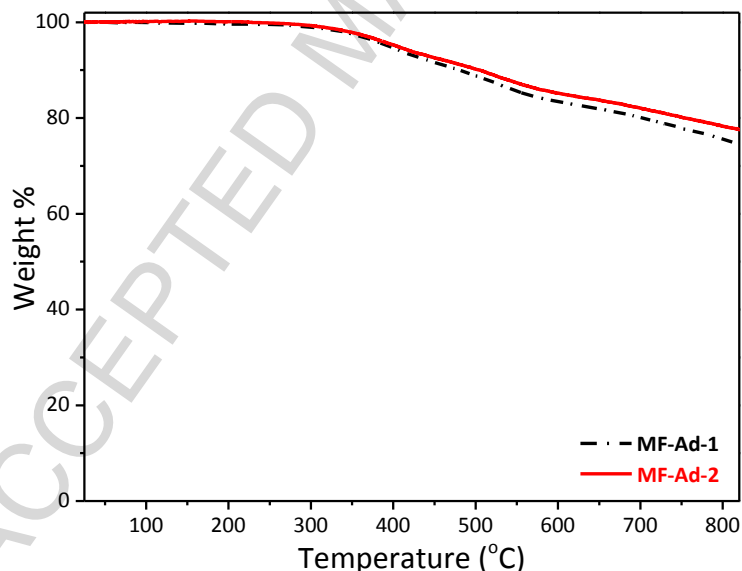


Figure 3. TGA profiles of **MF-Ad-1** and **MF-Ad-2**.

The porosity of the **MF-Ad** networks was determined by N_2 adsorption at 77 K. As illustrated in Figure 4 (a), the adsorption-desorption isotherms of **MF-Ad-1** and **MF-Ad-2** were very similar, both giving rise to type I isotherms, according to the IUPAC classification[13]. The sharp uptake at relatively low pressures ($p/p_0 < 0.0001$) demonstrated the microporosity of the frameworks in line with previous reports[6]. The hysteresis loop in the desorption isotherm is mostly attributed to the swelling of the frameworks or the interstitial voids between polymeric particles[22, 23]. Moreover, both of the narrow hysteresis loops and the consecutive N_2 uptake at higher relative pressures (1.0 bar) indicated the existence of interparticle void spaces or macropores within the frameworks. The Brunauer-Emmett-Teller (BET) surface area of **MF-Ad-1** and **MF-Ad-2** was evaluated to be 536 and 642 $m^2 g^{-1}$, respectively. The low BET surface area in our systems may be attributed to the large space effect of adamantane in the knots, HBPBA and TBBPA, as compared to reported non-adamantane-based microporous organic polymer, which exhibited higher BET surface area[24-26].

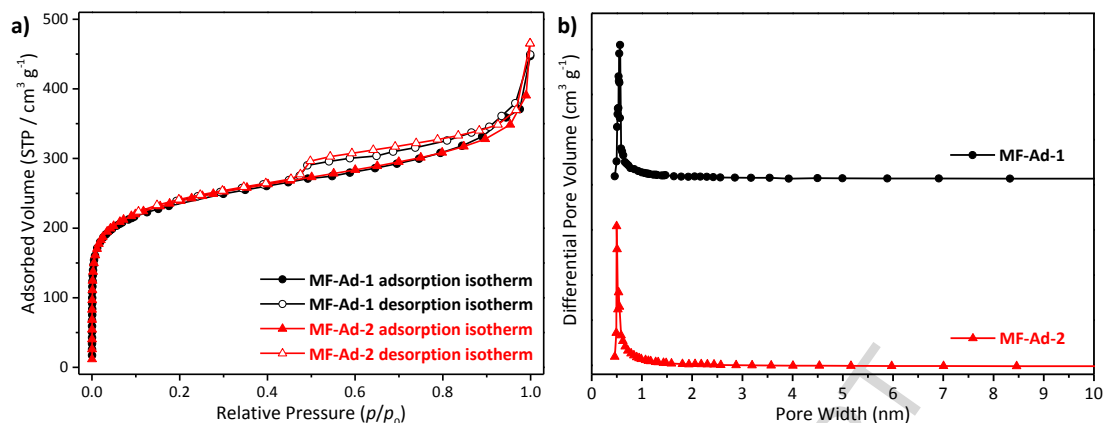


Figure 4. (a) N_2 sorption isotherms of **MF-Ad-1** and **2** at 77.3 K and (b) pore size distribution for **MF-Ad-1** and **2**.

Nonlocal density functional theory (NLDFT) was used to investigate pore size distribution (PSD) of these two **MF-Ad** networks. According to Figure 4 (b), **MF-Ad** networks exhibited abundant ‘ultra-microporous’ structures, where microporous diameters dominated at around 0.57 and 0.49 nm for **MF-Ad-1** and **MF-Ad-2**, respectively. Moreover, the microporosity ($V_{\text{micro}}/V_{\text{total}}$) at a relative pressure of 1.0 bar was found to be 0.62 (62%) for **MF-Ad-1** and 0.65 (65%) for **MF-Ad-2**, in line with the PSD of the networks, indicating that the majority of the pores were in the microporous domain. The porous properties of these **MF-Ad** networks are summarized in Table 1.

Table 1. Surface area and porosity of the **MF-Ad** networks.

Networks	S_{BET}^a ($\text{m}^2 \text{g}^{-1}$)	S_{micro}^b ($\text{m}^2 \text{g}^{-1}$)	V_{total}^c ($\text{cm}^3 \text{g}^{-1}$)	V_{micro}^d ($\text{cm}^3 \text{g}^{-1}$)	$V_{\text{micro}}/V_{\text{total}}$	Pore Size ^e (nm)
MF-Ad-1	536	345	0.29	0.18	0.62	0.57
MF-Ad-2	642	444	0.34	0.22	0.65	0.49

^a Calculated using the Brunauer-Emmett-Teller (BET) method.

^b Microporous surface area calculated using the *t*-plot method.

^c Total pore volume calculated at $p/p_0 = 1.0$.

^d Micropore volume calculated at $p/p_0 = 1.0$.

^e Pore size distributions obtained by NLDFT method.

3.3 Gas transport properties

Inspired by the relatively high surface area of our **MF-Ad** networks, the small gas (such as CO_2 , CH_4 and N_2) storage properties and selective uptake were evaluated at 273 K and 298 K with the pressure at 0 - 1.0 bar, as shown in Figure 5 and Table 2. **MF-Ad-2** exhibited the highest CO_2 uptake capacity (was up to $72.5 \text{ cm}^3 \text{g}^{-1}$) at 273 K / 1.0 bar, and $36.5 \text{ cm}^3 \text{g}^{-1}$ at 298 K / 1.0 bar. For comparison, the CO_2 uptake capacity of **MF-Ad-2** surpassed most previously reported polymeric organic frameworks (POFs) with higher BET surface area in the same conditions, such as pyridine-based functional conjugated microporous polymer (PCMP-1, $55.6 \text{ cm}^3 \text{g}^{-1}$, $S_{\text{BET}} = 1136 \text{ m}^2 \text{g}^{-1}$)[27] polyhedral oligomeric silsesquioxane microporous polymer (PMOP-1, $58.0 \text{ cm}^3 \text{g}^{-1}$, $S_{\text{BET}} = 806 \text{ m}^2 \text{g}^{-1}$)[28], hyper-crosslinked aromatic polymer (NOP-47, $67.2 \text{ cm}^3 \text{g}^{-1}$, $S_{\text{BET}} = 1246 \text{ m}^2 \text{g}^{-1}$)[29]. Moreover, the values exceed several reported microporous polymers based on a adamantane, which exhibited similar BET surface areas, such as, tetraphenyladamantane-based polyimide (API-6FA, $63.1 \text{ cm}^3 \text{g}^{-1}$, $S_{\text{BET}} = 752 \text{ m}^2 \text{g}^{-1}$)[25], tetraphenylethene-based microporous polymer (TPE-AD, $40.1 \text{ cm}^3 \text{g}^{-1}$, $S_{\text{BET}} = 615 \text{ m}^2 \text{g}^{-1}$)[30]. The comparable, or superior, CO_2 uptake capacities of these two **MF-Ad** networks is attributed to the combination of an ‘ultra-microporous’ structure with conventional microporosity, where a narrow pore size distribution can enhance the affinity between small gas and networks, resulting in high adsorption capacity[14, 31]. Interestingly, more reactive sites on bulky cyclic aliphatic (six or eight) adamantanes may produce less topological defects, which would result in narrower pore size distribution [32, 33]. Moreover, the physisorption isotherms had not reached saturation state at 1.0 bar. This result suggests that higher capacities can be obtained at increased pressures.

The isosteric heat of adsorption (Q_{st}) of these two frameworks were calculated from the Clausius-Clapeyron equation based on the CO_2 adsorption branches at 273 K and 298 K. The Q_{st} values were 32.2 and 36.7 kJ mol^{-1} at zero-coverage (Table 2 and Figure S6, ESI). The Q_{st} values were much higher than those previously reported microporous frameworks, to name a few, thiadiazole-functionalized covalent organic framework (TH-COF-1, 31 kJ

mol⁻¹)[34], borazine-linked polymers (BLPs, 20.2 - 28.3 kJ mol⁻¹)[35, 36] and metalloporphyrin-based microporous covalent triazine framework (MCTF-300-500, 24.6 - 26.3 kJ mol⁻¹)[37]. The high Q_{st} of two **MF-Ads** can be presumably attributed to the existence of abundant microporous, especially the 'ultra-microporous' structure [Figure 2 and Figure 4 (b)], which would enhance the binding affinity between the frameworks and CO₂ molecules[29, 38].

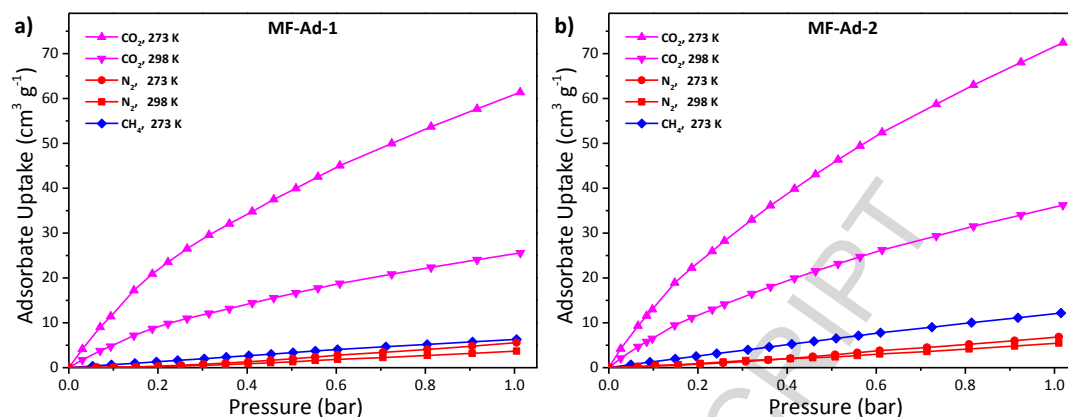


Figure 5. Adsorption isotherms of CO₂, CH₄ and N₂ in **MF-Ad-1** (a) and **MF-Ad-2** (b) at 273 K.

On the other hands, the adsorption selectivity is one of the most crucial parameters for microporous frameworks in CO₂ capture and sequestration (CCS). Herein, the adsorption selectivities of CO₂ over N₂ or CH₄ were assessed using Henry's law at low pressure (Figure S7, ESI)[39]. As showed in Table 2, both **MF-Ad-1** and **MF-Ad-2** displayed much higher CO₂/N₂ selectivities (59.1 and 23.9) than CO₂/CH₄ (6.9 and 3.9), owing to the larger quadrupole moment of CO₂ (13.4×10^{-40} C m²) over N₂ (4.7×10^{-40} C m²), and nonpolar CH₄[40, 41]. Additionally, CO₂ has much a higher critical temperature than CH₄ and N₂, which allows it to be easily adsorbed into the narrow pores[39].

The selectivity values for CO₂/N₂ were also comparable with most functional microporous polymers reported in the literature (Table S1, ESI)[14, 38, 42-45]. Interestingly, most reported functional microporous polymers possess excellent CO₂ uptake capacity but low selectivities for CO₂/N₂, which could be due to the presence of heteroatoms in the framework (absent in our materials), which not only aid CO₂ capture, but also N₂. On the other hand, in spite of higher CH₄ uptake capacity for each network than N₂, it is clearly seen that the selectivity of CO₂/CH₄ is much lower than CO₂/N₂ because of the higher polarizability of CH₄ in comparison to N₂[46, 47].

Table 2. The gas uptake capacities (cm³ g⁻¹) of the networks at 273 K (298 K) and 1.0 bar.

Networks	CO ₂ uptake		N ₂ uptake		CH ₄ uptake	Selectivity ^a		Q_{st} CO ₂ [kJ mol ⁻¹] ^b
	273 K	298 K	273 K	298 K	273 K	CO ₂ /N ₂	CO ₂ /CH ₄	
MF-Ad-1	51.2	25.6	4.6	3.7	5.3	59.1	6.9	32.2
MF-Ad-2	72.5	36.5	6.8	5.3	12.2	23.9	3.9	36.7

^a Adsorption selectivity based on the Henry's law.

^b Q_{st} CO₂ was calculated from CO₂ isotherms collected at 273 K and 298 K at zero-coverage.

3.4 Preparation and performance of the MF-Ad films

Microporous organic frameworks possess excellent hydrothermal stability. However, to date, as they have been limited to the being amorphous powders with poor processability, there remains a key bottleneck that hamper real world application of such microporous polymers. To address this fundamental constraint, herein, films based on stainless steel meshes have been fabricated by physically binding **MF-Ad** and PDMS to the metal scaffold. The water contact angle (CA) of these stainless-steel mesh films reached 163 ° and 165 ° for **MF-Ad-1** and **MF-Ad-2**, respectively, while the stainless-steel mesh films of pure PDMS films attained 138 ° (Figure S8, ESI). These results demonstrate that the two as-prepared **MF-Ad** coated meshes possess excellent superhydrophobic or superoleophilic properties (water CA > 150 °).

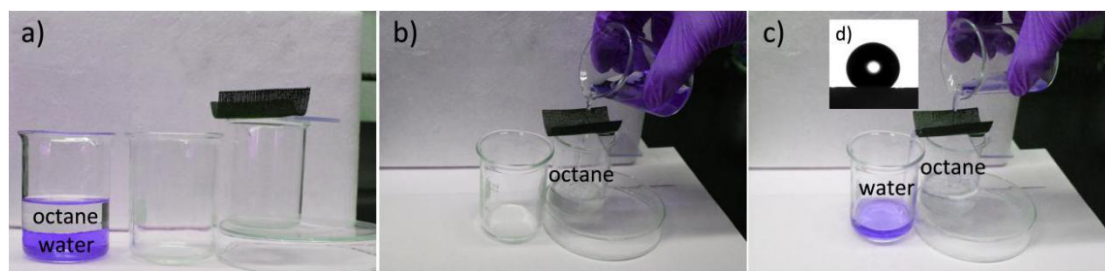


Figure 6. The separation of octane/water mixture using **MF-Ad-2**.

Additionally, these **MF-Ad**-based films exhibited excellent affinity for the organic component (such as diesel, octane, chloroform) of aqueous-organic solvent mixtures (20.0 ml for each). Taking **MF-Ad-2** based mesh as an example, for the mixture of DI water and octane, the octane (colorless in the images in Figure 6) penetrated through the mesh directly while the DI water (dyed purple with rhodamine B, 0.2 g rhodamine B in 20 mL DI water) stayed on the surface of the mesh and could be poured off easily separated from the organic phase, as depicted in Figure 6. Similar results were observed in the separation of chloroform/water and diesel/water mixtures (Figure S9, ESI). As expected from the results reported herein, the **MF-Ad-2** based mesh exhibited the most superior performance of 'oil'/water separation, while, conversely, for PDMS films (without **MF-Ad**), both water and octane penetrated the mesh and were not separated. The **MF-Ad-2** separation efficiency was 99.6 % for the octane/water mixture (calculated using a previously reported method, Equation S1, ESI)[48]. After recycling 5 times, the separation efficiency did not vary significantly, highlighting the excellent reusability of these materials (Figure S10, ESI). In short, these findings inspire the expansion in application of such microporous polymers, particularly those with excellent gas capture/selectivity performance, but poor processability as a consequence of their extensively crosslinked framework.

4. Conclusions

In summary, two novel **MF-Ad-1** and **MF-Ad-2** frameworks based on adamantane were designed and developed and have been shown to possess ultra-high thermochemical stabilities. With high surface area and ultra-microporous structure, these **MF-Ad** networks exhibited significantly superior gas permeability, with CO_2/N_2 and CO_2/CH_4 selectivities up to 59.1 and 6.9, respectively. Based on their hydrophobic nature, the water CA of **MF-Ad-1** and **MF-Ad-2** films were up to 163° and 165° . Furthermore, after coating the **MF-Ad-2** powder on a stainless-steel mesh (with PDMS as a binder), the **MF-Ad**-based mesh was shown to separate water and octane or water and chloroform or water and diesel instantly, with high separation efficiency (up to 97.8 % for the separation of water and octane) after repeating for at least 5 cycles. We anticipate that this work will inspire the extension of application of these (and similar) functional microporous polymers, particularly in oil/water separation.




Acknowledgments

This work was supported by National Natural Science Foundation of China (No. 21476051), Science and Technology Program of Guangdong Province (No. 2016A050502057), Science and Technology Program of Guangzhou City (No. 201704030075 and No. 201604010015) and Natural Science Foundation of Guangdong Province (No. 2016A030310349). PDT thanks the State Administration for Foreign Experts Affairs and the Royal Society of Chemistry for a Visiting Researcher Programme grant to China.

References

- [1] S.K. Kundu, A. Bhaumik, Novel Nitrogen and Sulfur Rich Hyper-Cross-Linked Microporous Poly-Triazine-Thiophene Copolymer for Superior CO₂ Capture, *ACS Sustainable Chemistry & Engineering*, 4 (2016) 3697-3703.
- [2] U. Diaz, A. Coma, Ordered covalent organic frameworks, COFs and PAFs. From preparation to application, *Coord Chem Rev*, 311 (2016) 85-124.
- [3] M. Pera-Titus, Porous Inorganic Membranes for CO₂ Capture: Present and Prospects, *Chem Rev*, 114 (2014) 1413-1492.
- [4] J.R. Li, R.J. Kuppler, H.C. Zhou, Selective gas adsorption and separation in metal-organic frameworks, *Chemical Society Reviews*, 38 (2009) 1477-1504.
- [5] S.Y. Ding, W. Wang, Covalent organic frameworks (COFs): from design to applications, *Chem Soc Rev*, 42 (2013) 548-568.
- [6] S.N. Talapaneni, D. Kim, G. Barin, O. Buyukcakir, S.H. Je, A. Coskun, Pillar[5]arene Based Conjugated Microporous Polymers for Propane/Methane Separation through Host-Guest Complexation, *Chem Mater*, 28 (2016) 4460-4466.
- [7] R. Dawson, A.J. Cooper, D.J. Adams, Nanoporous organic polymer networks, *Progress in Polymer Science*, 37 (2012) 530-563.
- [8] J.W. Li, Y.W. Ren, C.R. Qi, H.F. Jiang, A chiral salen-based MOF catalytic material with high thermal, aqueous and chemical stabilities, *Dalton T*, 46 (2017) 7821-7832.
- [9] N. Manoranjana, S.I. Woo, Synthesis of azo linked polymers by a diazotization-coupling reaction and its application for CO₂ capture, *Rsc Adv*, 6 (2016) 93463-93468.
- [10] S. Dey, A. Bhunia, I. Boldog, C. Janiak, A mixed-linker approach towards improving covalent triazine-based frameworks for CO₂ capture and separation, *Micropor Mesopor Mat*, 241 (2017) 303-315.
- [11] H. Lim, J.Y. Chang, Preparation of Clickable Microporous Hydrocarbon Particles Based on Adamantane, *Macromolecules*, 43 (2010) 6943-6945.
- [12] S. Zulfiqar, D. Mantione, O. El Tall, M.I. Sarwar, F. Ruiperez, A. Rothenberger, D. Mecerreyes, Nanoporous amide networks based on tetraphenyladamantane for selective CO₂ capture, *J Mater Chem A*, 4 (2016) 8190-8197.
- [13] X. Li, J.W. Guo, H.B. Yue, J.W. Wang, P.D. Topham, Synthesis of thermochemically stable tetraphenyladamantane-based microporous polymers as gas storage materials, *Rsc Adv*, 7 (2017) 16174-16180.
- [14] M.G. Rabbani, T. Islamoglu, H.M. El-Kaderi, Benzothiazole- and benzoxazole-linked porous polymers for carbon dioxide storage and separation, *J Mater Chem A*, 5 (2017) 258-265.
- [15] R. Du, Q. Zhao, Z. Zheng, W. Hu, J. Zhang, 3D Self-Supporting Porous Magnetic Assemblies for Water Remediation and Beyond, *Adv Energy Mater*, 6 (2016) 1600473.
- [16] Y. Lim, M.C. Cha, J.Y. Chang, Compressible and monolithic microporous polymer sponges prepared via one-pot synthesis, *Sci Rep*, 5 (2015) 15957.
- [17] W.J. Fan, X.F. Liu, Z. Zhang, Q.J. Zhang, W. Ma, D.Z. Tan, A. Li, Conjugated microporous polymer nanotubes and hydrophobic sponges, *Micropor Mesopor Mat*, 196 (2014) 335-340.
- [18] A. Li, H.X. Sun, D.Z. Tan, W.J. Fan, S.H. Wen, X.J. Qing, G.X. Li, S.Y. Li, W.Q. Deng, Superhydrophobic conjugated microporous polymers for separation and adsorption, *Energ Environ Sci*, 4 (2011) 2062-2065.
- [19] J.W. Guo, X.F. Lai, S.Q. Fu, H. Yue, J.W. Wang, P.D. Topham, Microporous organic polymers based on hexaphenylbiadamantane: Synthesis, ultra-high stability and gas capture, *Mater Lett*, 187 (2017) 76-79.
- [20] O. Buyukcakir, S.H. Je, S.N. Talapaneni, D. Kim, A. Coskun, Charged Covalent Triazine Frameworks for CO₂ Capture and Conversion, *ACS Appl Mater Interfaces*, 9 (2017) 7209-7216.
- [21] J.X. Jiang, F. Su, A. Trewin, C.D. Wood, N.L. Campbell, H. Niu, C. Dickinson, A.Y. Ganin, M.J. Rosseinsky, Y.Z. Khimyak, A.I. Cooper, Conjugated microporous poly(aryleneethynylene) networks, *Angew Chem Int Edit*, 46 (2007) 8574-8578.
- [22] J. Weber, A. Thomas, Toward stable interfaces in conjugated polymers: Microporous poly(p-phenylene) and poly(phenyleneethynylene) based on a spirobifluorene building block, *J Am Chem Soc*, 130 (2008) 6334-6335.
- [23] M. Saleh, H.M. Lee, K.C. Kemp, K.S. Kim, Highly Stable CO₂/N₂ and CO₂/CH₄ Selectivity in Hyper-Cross-Linked Heterocyclic Porous Polymers, *ACS Appl Mater Inter*, 6 (2014) 7325-7333.
- [24] Y. Yuan, F. Sun, H. Ren, X. Jing, W. Wang, H. Ma, H. Zhao, G. Zhu, Targeted synthesis of a porous aromatic framework with a high adsorption capacity for organic molecules, *J Mater Chem*, 21 (2011) 13498-13502.
- [25] G.Y. Li, B. Zhang, J. Yan, Z.G. Wang, Microporous polyimides with functional groups for the adsorption of carbon dioxide and organic vapors, *J Mater Chem A*, 4 (2016) 11453-11461.
- [26] D.-P. Liu, Q. Chen, Y.-C. Zhao, L.-M. Zhang, A.-D. Qi, B.-H. Han, Fluorinated Porous Organic Polymers via Direct C-H Arylation Polycondensation, *ACS Macro Letters*, 2 (2013) 522-526.
- [27] J.K. Zang, Z.Q. Zhu, H.X. Sun, W.D. Liang, A. Li, Synthesis of functional conjugated microporous polymers

- containing pyridine units with high BET surface area for reversible CO₂ storage, *React Funct Polym*, 99 (2016) 95-99.
- [28] J. Liu, Y.F. Liu, X.W. Jiang, Y.L. Luo, Y.N. Lyu, POSS-based microporous polymers: Efficient Friedel-Crafts synthesis, CO₂ capture and separation properties, *Micropor Mesopor Mat*, 250 (2017) 203-209.
- [29] D.Y. Chen, S. Gu, Y. Fu, X.B.A. Fu, Y.D. Zhang, G.P. Yu, C.Y. Pan, Hyper-crosslinked aromatic polymers with improved microporosity for enhanced CO₂/N₂ and CO₂/CH₄ selectivity, *New J Chem*, 41 (2017) 6834-6839.
- [30] H. Lee, H.W. Park, J.Y. Chang, Preparation of microporous polymers consisting of tetraphenylethene and alkyne units, *Macromolecular Research*, 21 (2013) 1274-1280.
- [31] C. Zhang, X. Yang, Y. Zhao, X. Wang, M. Yu, J.-X. Jiang, Bifunctionalized conjugated microporous polymers for carbon dioxide capture, *Polymer*, 61 (2015) 36-41.
- [32] M.M. Traudafir, L. Pop, N.D. Hadade, M. Florea, F. Neatu, C.M. Teodorescu, B. Duraki, J.A. van Bokhoven, I. Grosu, V.I. Parvulescu, H. Garcia, An adamantane-based COF: stability, adsorption capability, and behaviour as a catalyst and support for Pd and Au for the hydrogenation of nitrostyrene, *Catal Sci Technol*, 6 (2016) 8344-8354.
- [33] H. Yu, C.J. Shen, Z.G. Wang, Micro- and Mesoporous Polycyanurate Networks Based on Triangular Units, *Chempluschem*, 78 (2013) 498-505.
- [34] L.Y. Wang, B. Dong, R.L. Ge, F.X. Jiang, J.H. Xiong, Y.N. Gao, J.K. Xu, A thiadiazole-functionalized covalent organic framework for efficient CO₂ capture and separation, *Micropor Mesopor Mat*, 224 (2016) 95-99.
- [35] T.E. Reich, S. Behera, K.T. Jackson, P. Jena, H.M. El-Kaderi, Highly selective CO₂/CH₄ gas uptake by a halogen-decorated borazine-linked polymer, *J Mater Chem*, 22 (2012) 13524-13528.
- [36] K.T. Jackson, M.G. Rabbani, T.E. Reich, H.M. El-Kaderi, Synthesis of highly porous borazine-linked polymers and their application to H₂, CO₂, and CH₄ storage, *Polym Chem-Uk*, 2 (2011) 2775-2777.
- [37] X.M. Liu, H. Li, Y.W. Zhang, B. Xu, A. Sigen, H. Xia, Y. Mu, Enhanced carbon dioxide uptake by metalloporphyrin-based microporous covalent triazine framework, *Polym Chem-Uk*, 4 (2013) 2445-2448.
- [38] Y.F. Xu, D. Chang, S. Feng, C. Zhang, J.X. Jiang, BODIPY-containing porous organic polymers for gas adsorption, *New J Chem*, 40 (2016) 9415-9423.
- [39] C.J. Shen, J. Yan, G.Y. Deng, B.A. Zhang, Z.G. Wang, Synthetic modulation of micro- and mesopores in polycyanurate networks for adsorptions of gases and organic hydrocarbons, *Polym Chem-Uk*, 8 (2017) 1074-1083.
- [40] M. Saleh, S.B. Baek, H.M. Lee, K.S. Kim, Triazine-Based Microporous Polymers for Selective Adsorption of CO₂, *J Phys Chem C*, 119 (2015) 5395-5402.
- [41] M. Saleh, J.N. Tiwari, K.C. Kemp, M. Yousuf, K.S. Kim, Highly Selective and Stable Carbon Dioxide Uptake in Polyindole-Derived Microporous Carbon Materials, *Environ Sci Technol*, 47 (2013) 5467-5473.
- [42] R. Bera, M. Ansari, S. Mondal, N. Das, Selective CO₂ capture and versatile dye adsorption using a microporous polymer with triptycene and 1,2,3-triazole motifs, *Eur Polym J*, 99 (2018) 259-267.
- [43] H.J. Zhang, C. Zhang, X.C. Wang, Z.X. Qiu, X.M. Liang, B. Chen, J.W. Xu, J.X. Jiang, Y.D. Li, H. Li, F. Wang, Microporous organic polymers based on tetraethynyl building blocks with N-functionalized pore surfaces: synthesis, porosity and carbon dioxide sorption, *Rsc Adv*, 6 (2016) 113826-113833.
- [44] X.Y. Wang, Y. Zhao, L.L. Wei, C. Zhang, J.X. Jiang, Nitrogen-rich conjugated microporous polymers: impact of building blocks on porosity and gas adsorption, *J Mater Chem A*, 3 (2015) 21185-21193.
- [45] T. Ratvijitvech, R. Dawson, A. Laybourn, Y.Z. Khimyak, D.J. Adams, A.J. Cooper, Post-synthetic modification of conjugated microporous polymers, *Polymer*, 55 (2014) 321-325.
- [46] J.W. Zhang, M.C. Hu, S.N. Li, Y.C. Jiang, Q.G. Zhai, Microporous rod metal-organic frameworks with diverse Zn/Cd-triazolate ribbons as secondary building units for CO₂ uptake and selective adsorption of hydrocarbons, *Dalton T*, 46 (2017) 836-844.
- [47] P. Arab, M.G. Rabbani, A.K. Sekizkardes, T. Islamoglu, H.M. El-Kaderi, Copper(I)-Catalyzed Synthesis of Nanoporous Azo-Linked Polymers: Impact of Textural Properties on Gas Storage and Selective Carbon Dioxide Capture, *Chem Mater*, 26 (2014) 1385-1392.
- [48] Q.M. Pan, M. Wang, H.B. Wang, Separating small amount of water and hydrophobic solvents by novel superhydrophobic copper meshes, *Appl Surf Sci*, 254 (2008) 6002-6006.

 Oil  Water  CO₂  N₂

Graphical abstract

ACCEPTED MANUSCRIPT